Biology of Reproduction, 2021, 104(6), 1292–1301
doi:10.1093/biolre/ioab048
Research Article
Advance Access Publication Date: 16 March 2021

OXFORD

Research Article

Sperm–oocyte signaling: the role of IZUMO1R and CD9 in PTK2B activation and actin remodeling at the sperm binding site†

Huizhen Wang[1], Xiaoman Hong[2] and William H. Kinsey[1,*]

[1]Department of Anatomy and Cell Biology, University of Kansas School of Medicine, Kansas City, KS, USA and [2]Department of Molecular and Integrative Physiology, University of Kansas School of Medicine, Kansas City, KS, USA

***Correspondence:** Department of Anatomy and Cell Biology, University of Kansas School of Medicine, Kansas City, KS 66160, USA. E-mail: wkinsey@kumc.edu

†Grant Support: This work was supported by NICHD-HD062860, and utilized core facilities supported by NICHD-HD02528 and HD090216.

Received 23 September 2020; Revised 9 February 2021; Accepted 15 March 2021

Abstract

Sperm–oocyte binding initiates an outside-in signaling event in the mouse oocyte that triggers recruitment and activation of the cytosolic protein kinase PTK2B in the cortex underlying the bound sperm. While not involved in gamete fusion, PTK2B activity promotes actin remodeling events important during sperm incorporation. However, the mechanism by which sperm–oocyte binding activates PTK2B is unknown, and the present study examined the possibility that sperm interaction with specific oocyte surface proteins plays an important role in PTK2B activation. Imaging studies revealed that as IZUMO1R and CD9 became concentrated at the sperm binding site, activated (phosphorylated) PTK2B accumulated in the cortex underlying the sperm head and in microvilli partially encircling the sperm head. In order to determine whether IZUMO1R and/or CD9 played a significant role in PTK2B recruitment and activation at the sperm binding site, the ability of oocytes null for *Izumo1r* or *Cd9*, to initiate an increase in PTK2B content and activation was tested. The results revealed that IZUMO1R played a minor role in PTK2B activation and had no effect on actin remodeling; however, CD9 played a very significant role in PTK2B activation and subsequent actin remodeling at the sperm binding site. These findings suggest the possibility that interaction of sperm surface proteins with CD9 or CD9-associated oocyte proteins triggers PTK2B activation at the sperm binding site.

Summary sentence

Sperm binding triggers PTK2B activation in the oocyte through a CD9-dependent mechanism.

Key words: fertilization, binding, *cd9*, *Izumo1r*, *Ptk2b*, actin.

Introduction

Fertilization in mammals involves a series of interactions between male and female gametes leading ultimately to sperm binding to and fusion with the oocyte. However, an equally important aspect of fertilization involves sperm incorporation, an actin-mediated event where elongating oocyte microvilli enhance contact with the sperm head [1, 2] and where localized remodeling of the cortical actin layer functions to draw the sperm head into the ooplasm [3]. The signal(s) that trigger sperm incorporation are not well understood, but recent work revealed that sperm interaction with the oocyte plasma membrane triggers a highly localized outside-in signaling event resulting in recruitment and activation (phosphorylation) of the protein tyrosine kinase 2 beta (PTK2B) in the oocyte cortex underlying the bound sperm. PTK2B kinase activity was found to play a significant role in actin remodeling at the sperm binding site, and to promote sperm incorporation [4]. Occurring even in the absence of sperm–oocyte fusion, PTK2B activation provided the first evidence that mammalian oocytes respond biochemically to sperm contact and raised the question of how the signal of sperm binding caused recruitment and activation of PTK2B. The goal of the present study was to identify specific oocyte proteins that function to transmit the signal(s) provided by bound sperm to drive PTK2B activation in the oocyte.

PTK2B is a member of the focal adhesion kinase family and can be activated in response to external stimuli acting through receptor tyrosine kinases [5], g-protein-linked receptors [6, 7], or integrin oligomerization [8, 9]. PTK2B performs a variety of functions in different cell types, including ion channel modulation [10], bone resorption [11], and actin-mediated events during lamellipodial activity [12–14], smooth muscle contraction [15, 16], and neuronal cell process formation [17]. Given the evidence that PTK2B can be activated by external stimuli, the approach in this study was to test whether oocyte membrane proteins that function in sperm binding were required for PTK2B activation. Sperm–oocyte binding involves trans-interactions between multiple proteins providing adhesive strength such that deletion of a single binding pair does not completely abolish sperm binding. Several known proteins that participate in sperm binding including $\alpha 6\beta 1$ and $\alpha 9\beta 1$ integrins [18, 19], as well as tetraspannins CD9 [20–22] and CD81 [23]. GPI-linked proteins have also been implicated in sperm binding [24] including the IZUMO1 receptor (IZUMO1R), which binds the sperm protein IZUMO with high specificity [25]. IZUMO1R and CD9 are of particular interest because, while oocytes null for either *Izumo1r* or *Cd9* can still bind sperm, they fail to fertilize oocytes and the knockout females are almost completely infertile [20, 25].

The objective of this study was to test the hypothesis that IZUMO1R and/or CD9 transmit a signal in response to sperm contact that triggers PTK2B activation and actin remodeling at the sperm binding site. The approach was to establish whether PTK2B was localized in the same region of the sperm binding site as IZUMO1R and CD9, then use knockout models to establish whether *Izumo1r* or *Cd9* was required for PTK2B activation. Oocytes from mice null for *Izumo1r* or *Cd9* were used for in vitro fertilization assays that were terminated during the early stages of sperm incorporation so that activated PTK2B could be detected. The activation state of PTK2B was quantified with an antibody to the phosphorylated "priming" site (Y^{402}), which is critical to PTK2B activation [26]. The quantification method used line scan analysis that measured fluorescence intensity in the plasma membrane and underlying cortical actin layer to allow comparison of changes in abundance of membrane proteins such as IZUMO1R and CD9 with the abundance of cytosolic proteins such as PTK2B as they become localized in the oocyte cortex. *Izumo1r*$^{-/-}$ oocytes retained a substantial capacity to activate PTK2B following sperm binding; however, PTK2B activation at *Cd9*$^{-/-}$ sperm binding sites was reduced to barely detectable levels and the ability to accumulate f-actin at the sperm binding site was also significantly reduced. These findings demonstrate that, in addition to a role in sperm binding, CD9 is required for PTK2B activation and actin remodeling at the sperm binding site.

Methods

Transgenic mice

Mouse sperm null for *Izumo1r* (*Izumo1r*$^{tm2a/tm2a}$) (Sanger institute, Cambridge, UK) and *Cd9*$^{-/-}$ sperm (*C57BL/6*$^{Cd\text{-}9\ tm1Osb}$ [20]) (Center for Animal Resources and Development, Kumamoto University, Japan) were used to fertilize oocytes from C57BL/6 females (Jackson Laboratory, Bar Harbor, ME) to produce heterozygotes that would be fertile. Following blastocyst transfer, heterozygotes were maintained as breeding colonies to produce *Izumo1r*$^{-/-}$ and *Cd9*$^{-/-}$ females, with *Izumo1r*$^{+/+}$ and *Cd9*$^{+/+}$ littermates, which were used as controls. Genotyping was performed as previously described [25, 27]. Experiments were conducted in accordance with the "Guide for the Care and use of Laboratory Animals" (Institute of Laboratory Animal Resources (U.S.) Committee on Care and Use of Laboratory Animals 1996; National Research Council (U.S.) 2011). Experimental procedures were approved by the University of Kansas Medical Center IACUC committee.

Gamete handling and in vitro fertilization

In vitro fertilization was carried out using *wt* B6D2F1/HSD (Envigo (Indianapolis, IN)) cauda epididymal sperm capacitated in FertiUp medium (KYD-005-EX, Cosmo Bio USA (Carlsbad, CA)) at 37°C and 5% CO_2 in air under mineral oil for 1 h. Oocytes were collected from females 4–5 weeks of age stimulated with 5 IU of Pregnant Mares Serum Gonadotropin (Sigma-Aldrich, St. Louis, MO) followed 48 h later by 5 IU human chorionic gonadotropin (hCG) (Sigma-Aldrich). Cumulus–oocyte complexes (COCs) were collected at 15–16 h post-hCG, washed in Flushing and Handling Medium (Specialty Media Inc., Phillipsburgh, NJ) containing 4 mg/ml BSA (FHM-BSA) (Sigma-Aldrich), then cumulus cells were removed by treatment with 30 IU/ml hyaluronidase (Sigma-Aldrich) for 10 min. Zona removal was performed by exposing oocytes to two consecutive 100 ul drops of Acid Tyrode's (Sigma-Aldrich), then transferred to 1 ml of FHM-BSA for pH neutralization. Zona-free eggs were washed into CARD medium (KYD-005-EX, Cosmo Bio USA (Carlsbad, CA)) and allowed to recover under oil for 1 h. Capacitated sperm were added to a final concentration of 2×10^4/ml and incubated under oil at 37°C and 5% CO_2 for in vitro fertilization. Animals were housed in a temperature and light cycle-controlled room.

Microscopy and image analysis

Oocytes with bound sperm were fixed in 2% formaldehyde with 1% saturated picric acid in PBS containing 40 uM phenylarsine oxide (Sigma-Aldrich) and 100 uM sodium ortho-vanadate (ThermoFisher Scientific, Waltham, MA) as phosphatase inhibitors. After fixation for 1 h, oocytes were processed for immunofluorescence as described and labelled with Hoechst 33342, rat anti-Folate Receptor 4 (IZUMO1R) (BioLegend, San Diego, CA), rat anti-CD9 (BD Pharmingen), or rabbit anti-phospho-PTK2B-Y^{402} (ThermoFisher,

Waltham, MA). Secondary antibodies include goat anti-rabbit Alexa Fluor 488 and goat anti-rat Alexa Fluor 555 (Thermofisher). Alexa Fluor 568 phalloidin (Thermofisher) was used to detect f-actin. All antibodies and dyes were used at a 1:200 dilution. The specificity of anti-IZUMO1R, anti-CD9 antibodies during immunofluorescence applications was demonstrated using *Izumo1r*$^{-/-}$ and *Cd9*$^{-/-}$ oocytes, while the specificity of anti-PTK2B-PY^{402} was tested in *wt* oocytes using a synthetic phosphopeptide duplicating the phosphorylation site at Y^{402} (ESDI {PY}AEIPD) from GenScript, Inc. Picastaway, NJ, USA (Supplementary Figure S1). Confocal microscopy was performed with a Nikon A1R microscope, using sequential scans with constant beam intensity. Images were recorded from *Z*-planes containing one or more sperm heads bound to the oocyte surface. Fluorescence associated with the oocyte plasma membrane and cortical actin layer was quantified in red, green, and blue channels by circumferential line scan (2 um wide) analysis using Metamorph 6.2 (Molecular Devices, Downington, PA and graphed using SigmaPlot 11 (SyStat Software, San Jose, CA)). The width of each sperm binding site was determined using inflection points in the blue channel corresponding to the Hoechst signal from sperm chromatin. The total fluorescence intensity within red and green channels was measured across the sperm binding site and expressed relative to baseline fluorescence calculated from a line drawn between the two inflection points representing adjacent cortex fluorescence intensity. Normalizing the binding site fluorescence intensity to the adjacent cortex within a *Z*-plane avoided the errors that result because of the image-wide differences in fluorescence intensity between *z*-planes at different distances from the excitation beam source. The integrated relative fluorescence intensity was used to provide a measure of IZUMO1R, CD9, PTK2B, PTK2B-PY^{402}, and actin content associated with each sperm binding site.

Expression of murine *cd9* in oocytes null for mouse *cd9*

The mouse *cd9* clone (# MG226288, ORIGENE (Rockville, MD)) was used to transfect *E. coli* (CopyCutter C400CH10, Lucigen Corporation (Middleton, WI)) and the sequence of the insert was confirmed. The plasmid was linearized with SacII (New England Biolabs, Ipswitch, MA) and in vitro transcription was performed with the mMessage mMachine T7 kit (ThermoFisher) after which RNA was purified with NUCAway spin column (ThermoFisher). Germinal vesicle-stage oocytes were isolated from mature follicles 45 h after stimulation of *Cd9*$^{-/-}$ females with 5 IU of PMSG. Cumulus–oocyte complexes (COCs) were cultured in FHM supplemented with 5% fetal bovine serum (F4135 Sigma-Aldrich) containing 10 uM milrinone (Sigma-Aldrich). mRNA encoding *Cd9* was injected into the granulosa-enclosed oocytes using a Xenoworks digital microinjector (Sutter Instruments Novato, CA) to achieve a final intracellular concentration of 0.35 ug/ml. COCs were transferred to 100 ul drops of CZB medium (EMD Millipore, Temecula, CA) containing 5% FBS and 10 uM milrinone under mineral oil and incubated for 90 min. Then oocytes were washed free of milrinone and cultured for 18 h at 37°C and 5% CO_2 in air. The matured oocytes were stripped of cumulus cells and zona pellucida as described above and incubated with capacitated *wt* sperm for 45 min to allow sperm binding.

Statistics

Data, in the form of integrated relative fluorescence intensity at sperm binding sites, were collected by repeated IVF experiments each of which used oocytes pooled from at least two females from the experimental and from the control group. Between 3 and 6 replicate experiments were done and the sperm binding site data were pooled within wt and experimental groups to calculate mean values. The statistical significance of differences in the mean relative integrated fluorescence intensity reporting PTK2B, PTK2B-PY^{402}, and f-actin at sperm binding sites was demonstrated using the Mann–Whitney rank sum test. Correlations between IZUMO1R and PTK2B-PY^{402} and CD9 and PTK2B-PY^{402} (Supplementary Figure S2) were determined with Pearson's correlation coefficient (Systat Software, San Jose, CA).

Results

Spatial relationship of IZUMO1R, CD9, and activated PTK2B at the sperm binding site

The different stages of PTK2B recruitment to the sperm binding site were reported earlier [4], and a similar analysis of the location and abundance of activated PTK2B (PTK2B-PY^{402}) at sperm binding sites is presented in Figure 1. PTK2B-PY^{402} was initially observed as a collection of small foci within the oocyte cortex and microvillar tips in close proximity to the sperm head (Figure 1A, B, E, F). The extent of PTK2B activation increased as the area of sperm contact with the oocyte expanded (Figure 1C and G), eventually forming a plaque underneath the sperm head (Figure 1D and H). During these early stages, IZUMO1R was also detected at the sperm binding site (Figure 1A–D), despite the fact that TX-100 used during immunolabeling extracted this GPI-linked protein from most of the oocyte plasma membrane. The distribution of IZUMO1R was similar to but not precisely colocalized with PTK2B-PY^{402} at the sperm binding site, with some sites enriched in IZUMO1R with no obvious PTK2B-PY^{402} present (Figure 1A) while other sites contained varying levels of both proteins (Figure 1B and C). In cases where the sperm head lay flat on the oocyte plasma membrane, IZUMO1R was usually in contact with the sperm head (46%, $n = 116$), but as reported elsewhere [28], IZUMO1R was often displaced to the edges of the sperm binding site (16%, $n = 116$) as IZUMO1R-IZUMO binding strength declined. In contrast, PTK2B-PY^{402} remained directly under the sperm head at this stage (Figure 1D).

CD9 is expressed in the oocyte plasma membrane and accumulates at sperm binding sites [29–31]. Analysis of oocytes between 10 and 20 min post-insemination (mpi) confirmed that CD9 was concentrated in the plasma membrane underneath bound sperm (Figure 1E, F, H) and in oocyte cell processes that extended onto the sperm head (Figure 1F and G). Some bound sperm were partially enveloped with multiple CD9-enriched oocyte processes (Figure 1F and G), while sperm that lay flat on the oocyte surface generally were in contact with CD9 only on one side (Figure 1H). Both CD9 and PTK2B-PY^{402} accumulated to some extent at most, but not all sperm binding sites (Figure 1E). Often the heaviest accumulation of CD9 and PTK2B-PY^{402} was seen in membrane structures extending from the oocyte surface to envelop the sperm (Figure 1F and G). Despite differences in co-localization, a moderate correlation was observed between IZUMO1R or CD9 abundance and PTK2B-PY^{402} abundance at sperm binding sites ($r = 0.531$ and 0.503, respectively, Supplementary Figure S2).

During later stages of sperm incorporation when the oocyte plasma membrane began to invaginate under the sperm head drawing it toward the ooplasm [32], IZUMO1R was no longer associated with the sperm binding site. In contrast, both CD9 and PTK2B-PY^{402} were concentrated at the site of invagination (Figure 2A).

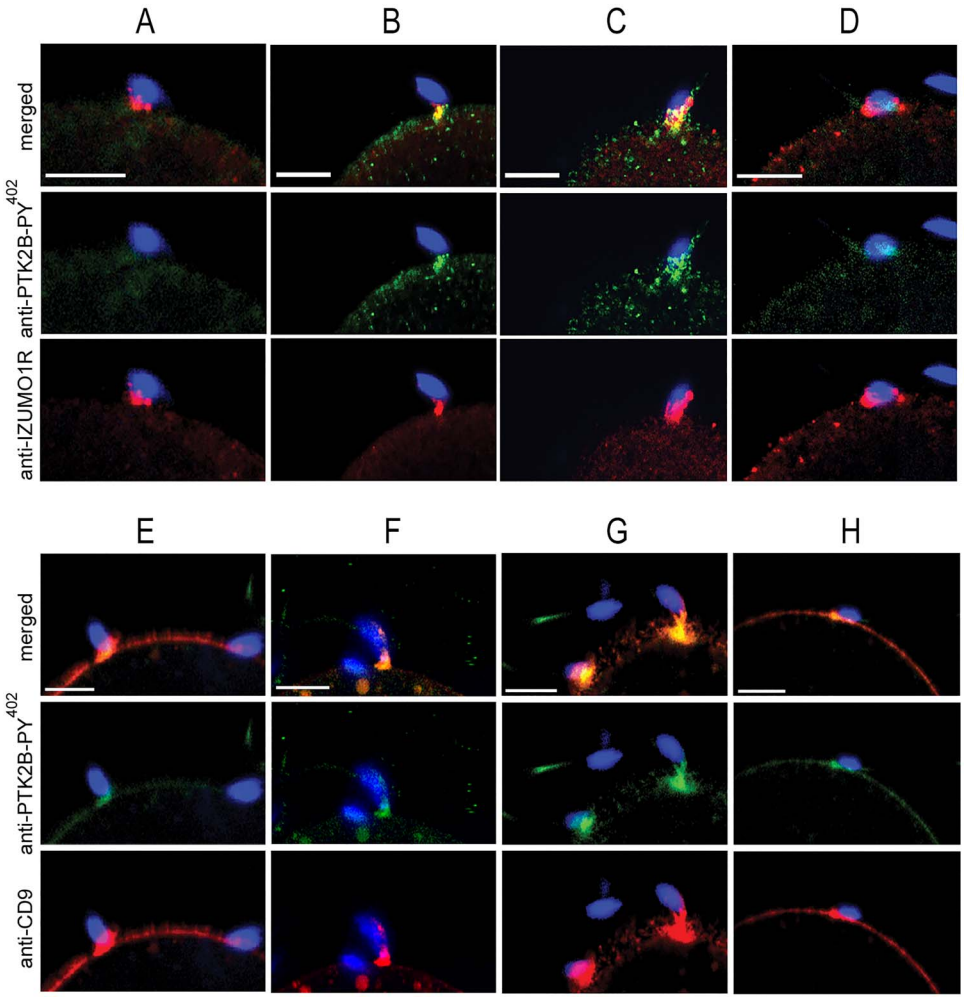

Figure 1. Progression of PTK2B-PY^{402}, IZUMO1R, and CD9 accumulation at sperm binding sites. Zona-free oocytes collected between 10 and 20 min post-insemination were prepared for immunofluorescence and labeled with anti-PTK2B-PY^{402} (green) and anti-IZUMO1R (red) (columns A-D) or with anti-PTK2B-PY^{402} and anti-CD9 (red) (columns E-H). Magnification is indicated by the bars, which represents 10 um.

As the sperm head was drawn into the ooplasm, CD9 and PTK2B-PY^{402} were displaced to the periphery of the sperm head (Figure 2B). Eventually, PTK2B-PY^{402} disappeared from the sperm incorporation site, while CD9 remained as a ring surrounding the incorporation site (Figure 2C).

Effect of IZUMO1R or CD9 ablation on PTK2B recruitment and activation at sperm binding sites

In order to determine whether IZUMO1R and/or CD9 play a significant role in PTK2B recruitment and activation at the sperm binding site, the ability of *Izumo1r*$^{-/-}$ and *Cd9*$^{-/-}$ oocytes to respond to *wt* sperm by recruiting PTK2B was compared to that of littermate *wt* oocytes. As seen in Figure 3, PTK2B accumulated in the cortex underlying *Izumo1r*$^{-/-}$ and *Cd9*$^{-/-}$ oocytes in a manner similar to that of *wt* oocytes. Quantification of PTK2B fluorescence was performed at each sperm binding site and was expressed relative to that of adjacent cortex. The increase in PTK2B fluorescence at *cd9*$^{-/-}$ binding sites was not significantly different than at *wt* binding sites (6.1% vs 7.8% ($P = 0.7$)); however, *Izumo1r*$^{-/-}$ binding sites exhibited significantly higher PTK2B fluorescence than *wt* and *cd9*$^{-/-}$ binding sites (26.6% vs 7.2% ($P < 0.001$)).

In contrast, the abundance of activated PTK2B-PY^{402} in *Izumo1r*$^{-/-}$ and *Cd9*$^{-/-}$ binding sites was different than the total PTK2B content. While *Izumo*1r$^{-/-}$ oocytes accumulated CD9 and PTK2B-PY^{402} at sperm binding sites in a pattern comparable to that of *wt* oocytes (Figure 4A), *Cd9*$^{-/-}$ oocytes exhibited little evidence of PTK2B-PY^{402} fluorescence at sperm binding sites. The relative integrated PTK2B-PY^{402} fluorescence associated with sperm binding sites from *wt* and *Izumo1r*$^{-/-}$ oocytes is seen in the bar graph (Figure 4B), and statistical analysis revealed that PTK2B-PY^{402} fluorescence at *Izumo1r*$^{-/-}$ binding sites was significantly lower (approximately half) than that of *wt* binding sites (Table 1). In contrast, the mean PTK2B-PY^{402} fluorescence intensity at *cd9*$^{-/-}$ sperm binding sites was much lower (approximately one-tenth) than that of *wt* sperm binding sites (Figure 4D). It is also apparent that in all lines examined, a subset of binding sites exhibited unusually high fluorescence intensities (greater than 100% above adjacent cortex), which is more easily seen in histogram format (Figure 4C and E). While *Izumo1r*$^{-/-}$ oocytes exhibited approximately half the number of "high-responding" binding sites as *wt* oocytes (22.8% vs 49%, Table 1), very few "high-responding" sperm binding sites were observed in *Cd9*$^{-/-}$ oocytes (0.4% vs 27.6%, Table 1).

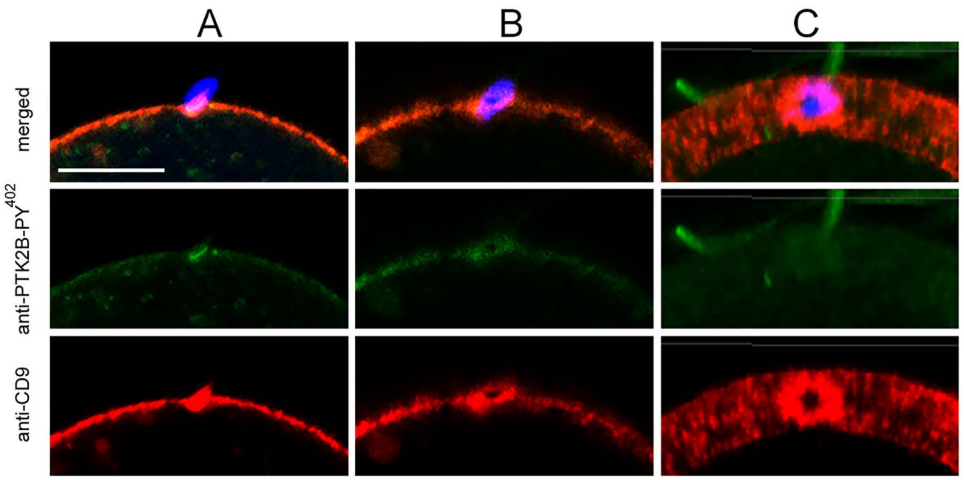

Figure 2. Changes in the distribution of PTK2B-PY^{402} and CD9 during early sperm incorporation. Zona-free *wt* oocytes were collected between 20 and 30 mpi and labelled with anti-PTK2B-PY^{402} (green) and anti-CD9 (red). Column A represents an "early" stage where the sperm has deformed the oocyte cortex. Column B demonstrates a sperm that is being drawn into the oocyte. Column C is a volume view produced by z-stack images of a different binding site that demonstrates the ring-like distribution of CD9 and the near absence of PTK2B-PY^{402} as seen from "above". Magnification is indicated by the bar, which represents 10 um.

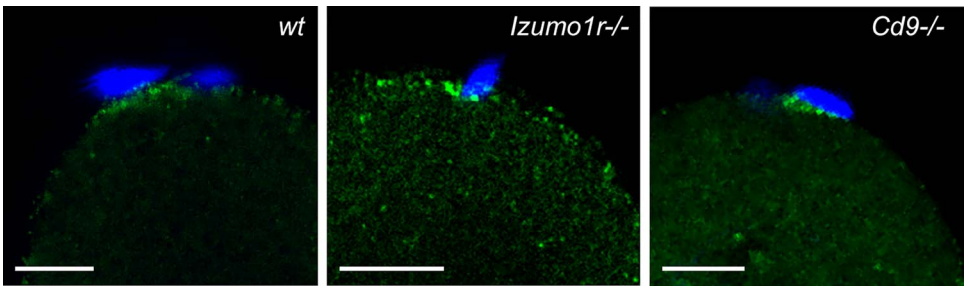

Figure 3. Effect of *Izumo1r* or *Cd9* ablation on PTK2B recruitment at sperm binding sites. Oocytes collected from *wt*, *Izumo1r*$^{-/-}$, or *Cd9*$^{-/-}$ females were incubated with capacitated sperm as above, fixed and labeled with anti-PTK2B (green). Magnification is indicated by the bars, which represents 10 um.

Table 1. Requirement for IZUMO1R and CD9 during PTK2B activation at sperm binding sites

Sperm	Oocytes	# Oocytes	# Binding sites analyzed	Mean integrated PTK2B-PY^{402} fluorescence	% binding sites >100% above baseline
wt	wt(Izumo*1r*$^{+/+}$)	34	192	138.1 ± 11.0%	49.0%
wt	*Izumo1r* $^{-/-}$	32	101	67.1 ± 9.1% (*)	22.8%
wt	*wt* (*Cd9*$^{+/+}$)	34	377	72.9 ± 6.7%	27.6%
wt	*Cd9* $^{-/-}$	32	266	7.7 ± 2.3% (*)	0.4%

The integrated relative fluorescence intensity of sperm binding sites was determined and the mean values are presented ±SEM. Data from the *wt* & *Izumo1r*$^{-/-}$ oocytes include 6 replicates, each from >3 females. Data from *wt* and *Cd9*$^{-/-}$ oocytes include 5 replicates, each from >3 females. (*) indicates a statistically significant difference between the mean in knockout oocytes and that of *wt* controls ($P \leq 0.001$).

In order to rule out potential pleiotropic effects of *Cd9* ablation, the ability of exogenous *cd9* expression to rescue the capacity of *Cd9*$^{-/-}$ oocytes to respond to sperm binding via phosphorylation of PTK2B-Y^{402} was tested. *Cd9*$^{-/-}$ oocytes were recovered at the germinal vesicle (GV) stage and then injected with mRNA encoding murine *c-Fyn*, or with injection buffer only as controls, while a third set was injected with mouse *Cd9* mRNA. After in vitro maturation and incubation with capacitated sperm, the oocytes with bound sperm were fixed and labeled with anti-CD9 and anti-PTK2B-PY^{402}. The *Cd9*$^{-/-}$ oocytes injected with *c-Fyn* mRNA or PBS did not express detectable CD9, and sperm binding sites exhibited little PTK2B-PY^{402} (Figure 5A). However, *Cd9*$^{-/-}$ oocytes injected with *Cd9* mRNA expressed mouse CD9 protein in the plasma membrane, often concentrated at sperm binding sites (Figure 5A), as well as concentrations of PTK2B-PY^{402} at sperm binding sites. The mean relative PTK2B-PY^{402} fluorescence intensity at sperm binding sites of oocytes injected with *Cd9* mRNA was significantly higher ($P \leq 0.01$) than that in the control group injected with *c-Fyn* mRNA (39.2 ± 3.4% vs 3.4 ± 1.2%) (Figure 5B and C). As observed in *wt* oocytes in earlier experiments (Figure 4E and G), the higher response to sperm binding

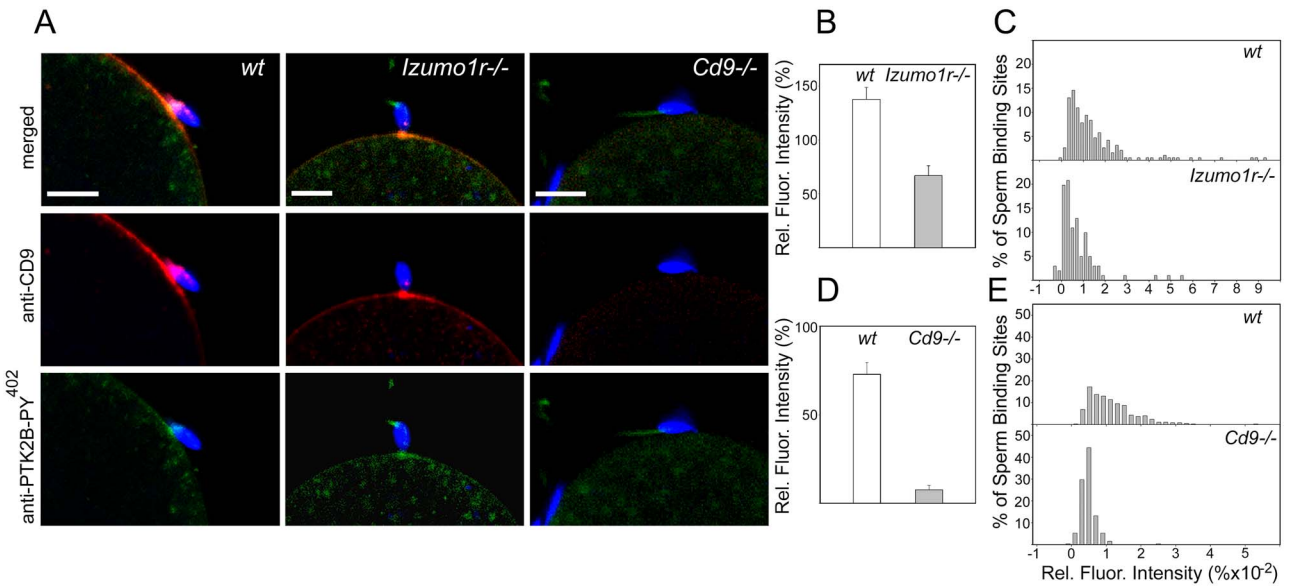

Figure 4. Effect of *Izumo1r* or *Cd*9 ablation on PTK2B phosphorylation at sperm binding sites. (A) Oocytes collected from *wt*, *Izumo1r* $^{-/-}$, or *Cd*9 $^{-/-}$ females were incubated with capacitated sperm, fixed and labeled with anti-PTK2B-PY^{402} (green) and anti-CD9 (red). Magnification is indicated by the bars, which represents 10 um. (B) The mean relative fluorescence intensity of PTK2B-PY^{402} at sperm binding sites of *wt* (white) and *Izumo1r*$^{-/-}$ oocytes (gray) from Table 1. (C) Percentage of *wt* and *Izumo1r*$^{-/-}$ sperm binding sites with increasing levels of PTK2B-PY^{402} fluorescence intensity relative to adjacent cortex. (D) The mean relative fluorescence intensity of PTK2B-PY^{402} at sperm binding sites of *wt* (white) and *Cd9*$^{-/-}$ oocytes (gray) from Table 1. (E) Percentage of *wt* and *Cd9*$^{-/-}$ sperm binding sites with increasing levels of PTK2B-PY^{402} fluorescence intensity relative to adjacent cortex.

by the *Cd9*$^{-/-}$ oocytes injected with *Cd9* mRNA was largely due to the presence of a group of "high responding sites" rather than to an increase in PTK2B-PY^{402} fluorescence at all sperm binding sites (Figure 5D).

Effect of IZUMO1R and CD9 ablation on f-actin accumulation at sperm binding sites.

Actin polymerization at the site of sperm–oocyte interaction has been reported in several species [1, 29, 33] and is thought to participate in enhancing the surface contact area between gametes and in subsequent sperm incorporation [34]. The observation that PTK2B suppression significantly reduced f-actin accumulation at sperm binding sites [4] indicated that PTK2B might play a significant role promoting actin remodeling in response to sperm interaction. In order to determine whether IZUMO1R or CD9 participates in induction of f-actin accumulation at the sperm binding site, the ability of *Izumo1r*$^{-/-}$ and *Cd9*$^{-/-}$ oocytes to respond to *wt* sperm via f-actin accumulation was tested. Both *wt* and *Izumo1r*$^{-/-}$ oocytes exhibited f-actin accumulation within elongated microvilli or filopodia and in the cortical actin layer under the sperm head (Figure 6A and B). Quantification of sperm binding site–associated f-actin fluorescence in *wt* and *Izumo1r*$^{-/-}$ oocytes revealed that the *Izumo1r*$^{-/-}$ oocytes were able to accumulate f-actin at the sperm binding site at levels similar to *wt* (Figure 6C and D) and statistical analysis revealed no significant difference in f-actin content in *wt* vs *Izumo1r*$^{-/-}$ binding sites (Table 2). In contrast, *Cd9*$^{-/-}$ oocytes appeared to be less active in accumulation of f-actin at sperm binding sites (Figure 6A, B, E, F) and statistical analysis (Table 2) demonstrated that the mean f-actin fluorescence at sperm binding sites of cd9$^{-/-}$ oocytes was significantly lower than that of *wt* oocytes. Our attempts to rescue f-actin accumulation by injecting *Cd9*$^{-/-}$ oocytes with *Cd9* mRNA were inconclusive, probably because *Cd9*$^{-/-}$ oocytes still have a substantial cortical actin layer, and the limited accumulation of CD9 following mRNA microinjection (while capable of detecting PTK2B phosphorylation against a low background) was unable to induce f-actin polymerization at a level detectable on top of the f-actin already present in the actin layer.

Taken together, the response of *Izumo1r*$^{-/-}$ oocytes to sperm binding involved lower PYK-PY^{402} content at the binding site than controls, but there was no difference in the level of f-actin accumulation at sperm binding sites. In contrast, sperm binding sites from *Cd9*$^{-/-}$ oocytes exhibited significantly lower (approximately one-tenth) PYK-PY^{402} content as well as significantly lower f-actin accumulation than in controls.

Discussion

Current understanding regarding interactions between mammalian sperm and oocytes has led to a model where oocyte membrane proteins such as IZUMO1R and CD9 interact specifically with sperm proteins such as IZUMO or possibly SPACA6 to initiate a high-affinity binding site [35, 36] that enables gamete fusion. During the sperm binding phase, the oocyte responds by formation of elongated, actin-containing microvilli that establish additional contacts with the sperm head, thereby increasing total surface contact area [37]. Subsequent actin-mediated events remodel the oocyte cortical actin layer and, as sperm and oocyte plasma membranes fuse, physically incorporate the sperm head into the ooplasm [32]. The stimuli that trigger these actin remodeling events in the oocyte have received little study, but the recent finding that PTK2B is recruited to the sperm binding site and that its activity supported actin remodeling and sperm incorporation [4] demonstrated that sperm–oocyte interaction could activate protein kinase–mediated outside-in signaling in the oocyte. PTK2B can respond to several different upstream events [38], but in some tissues, PTK2B is activated by interaction with plasma

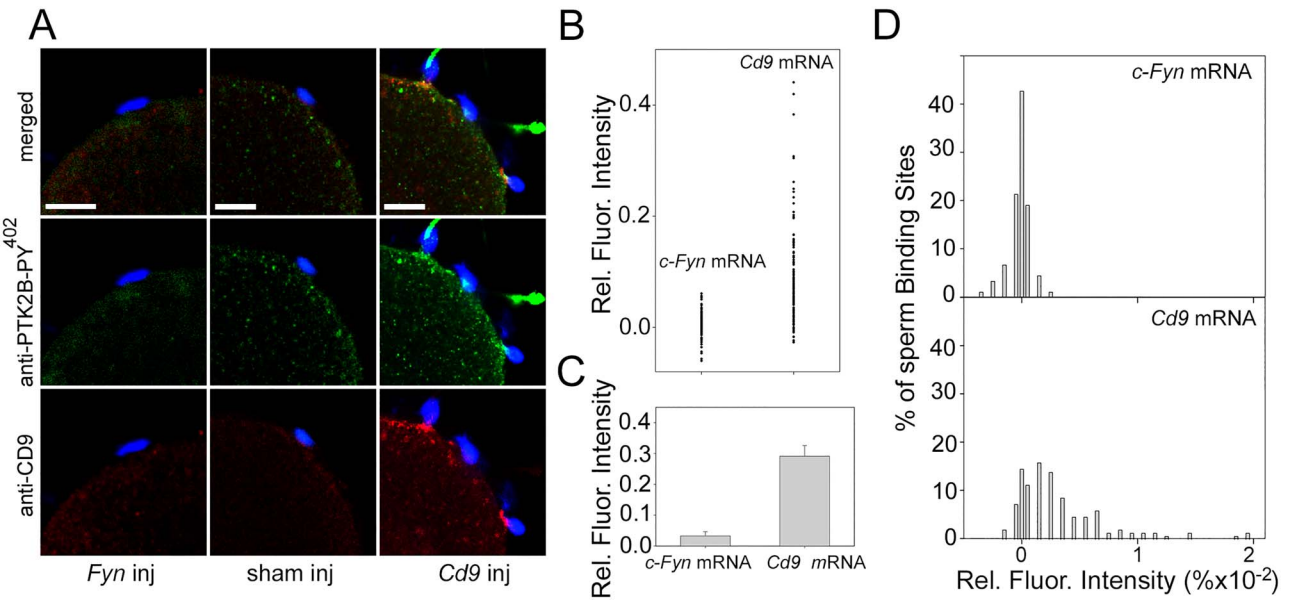

Figure 5. Rescue of *Cd9*$^{-/-}$ oocytes by injected *Cd*9 mRNA, GV stage oocytes from *Cd9*$^{-/-}$ females were injected with mRNA encoding *c-Fyn* (*c-Fyn* inj), with buffer only (sham inj), or with *Cd9* mRNA (*Cd9* inj) as described in "Methods". (A) Matured oocytes with bound sperm were fixed and labeled with anti-CD9 (red) and anti-PTK2B-PY^{402} (green). (B) Relative PTK2B-PY^{402} fluorescence intensity at sperm binding sites from *c-Fyn*-injected and *Cd9*-injected oocytes. (C) Mean PTK2B-PY^{402} fluorescence intensity at sperm binding sites from *c-Fyn*-injected and *Cd9*-injected oocytes ±SEM. (D) Histogram presentation of the percentage of sperm binding sites with increasing levels of PTK2B-PY^{402} fluorescence. Magnification is indicated by the bars, which represent 10 um. Data were obtained from 3 replicates, each from at least two females, totaling 16 oocytes in each group. The number of sperm binding sites examined included 89 from the c-*Fyn*-injected group and 151 from the cd9-injected group.

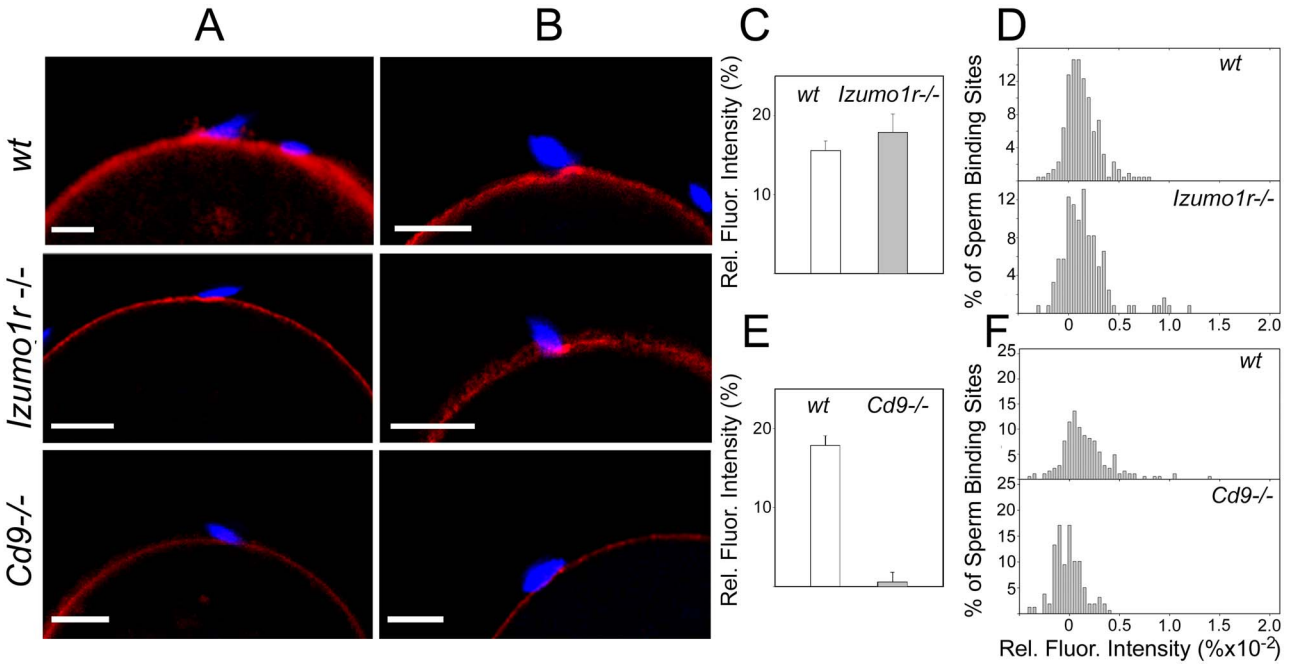

Figure 6. Effect of *Izumo1r* or *Cd*9 ablation on f-actin accumulation at sperm binding sites. Zona-free oocytes from *wt*, *Izumo1r*$^{-/-}$, or *Cd*9$^{-/-}$ females with bound sperm were fixed and labeled with alexa568-phalloidin (red) to detect f-actin. Columns A and B represent early stages of sperm-oocyte interaction. (C) Mean relative fluorescence intensity of f-actin at sperm binding sites of *wt* (white) and *Izumo1r*$^{-/-}$ oocytes (gray) from Table 2. (D) Histogram presentation of the percentage of *wt* and *Izumo1r*$^{-/-}$ sperm binding sites with increasing levels of PTK2B-PY^{402} fluorescence intensity relative to adjacent cortex. (E) The mean relative fluorescence intensity of f-actin at sperm binding sites of *wt* (white) and *Cd9*$^{-/-}$ oocytes (gray) from Table 2. (F) Percentage of *wt* and *Cd9*$^{-/-}$ sperm binding sites with increasing levels of PTK2B-PY^{402} fluorescence intensity relative to adjacent cortex. Magnification is indicated by the bar, which represents 10 um.

Table 2. Requirement of oocyte IZUMO1R and CD9 for actin accumulation at sperm binding sites

Sperm	Oocytes	# Oocytes	# Binding sites analyzed	Mean integrated f-actin fluorescence
wt	*wt*(Izumo*1r*$^{+/+}$)	22	219	15.6 ± 1.2%
wt	*Izumo1r*$^{-/-}$	37	122	17.9 ± 2.3%
wt	*wt* (*Cd9*$^{+/+}$)	16	184	17.9 ± 1.2%
wt	*Cd9*$^{-/-}$	18	158	0.6 ± 1.2% (*)

The integrated relative fluorescence intensity of sperm binding sites was determined and the mean values are presented ±SEM. Data from *wt*, *Izumo1r*$^{-/-}$ and *Cd9*$^{-/-}$ oocytes include 4 replicates, each from >3 females. (*) indicates a statistically significant difference between the mean of knockout oocytes from that of *wt* controls ($P \leq 0.001$).

membrane proteins following cell–cell or cell–matrix contact [8, 39], raising the possibility that interaction of sperm and oocyte surface proteins might induce activation of PTK2B. The objective of the present study was to determine whether oocyte proteins involved in sperm binding are required for PTK2B activation in the oocyte. While a number of oocyte proteins have been implicated in sperm binding, IZUMO1R and CD9 were selected for this study because their role in sperm binding has been well established and because oocytes null for *Izumo1r* or *Cd9* can bind sperm but do not progress further and are therefore infertile [20, 25]. The approach used was to determine whether these two membrane proteins were localized in close proximity to cytosolic PTK2B at the sperm binding site, and then to test whether expression of *Izumo1r* or *Cd9* was required for PTK2B activation.

Methodology

In order to quantify differences in the abundance of the membrane proteins IZUMO1R and CD9 as well as PTK2B and its activated form PTK2B-PY^{402}, line scan analysis was used to quantify antibodies bound to their specific targets using fluorescence-tagged secondary antibodies. The width of the measurement line was chosen to include the plasma membrane (containing IZUMO1R and CD9) and underlying cortical actin layer where the cytosolic protein PTK2B and PTK2B-PY^{402} were located. However, this limited resolution of plasma membrane specializations including changes in microvillus structure or membrane associated microvesicles. So, a change in fluorescence intensity might represent an increase in the concentration of a protein within the lipid bilayer or a change in the total membrane surface area within the sperm binding site. Likewise, this method does not have the resolution to assess membrane fusion; however, the amount of each protein associated with the binding site is represented fairly accurately relative to the adjacent cortex.

Spatial relationship between IZUMO1R, CD9, and PKY2-PY^{402} at the sperm binding site

IZUMO1R, a GPI-linked membrane protein, and the tetraspannin CD9 differ in their tertiary structure and in their distribution in the oocyte plasma membrane. IZUMO1R is distributed evenly on the oocyte surface of the mouse [25] and human [40] oocyte prior to fertilization. In contrast, CD9 is restricted to the microvillus-enriched domain of the mouse oocyte [29], is concentrated on microvilli [41, 42], and can be shed as microvesicles into the perivitelline space [37] where they can bind to the sperm head [31]. In contrast, IZUMO1R initially interacts directly with IZUMO at the equatorial segment region of the sperm, but as IZUMO undergoes self-dimerization, IZUMO1R is displaced to regions adjacent to the edges of the sperm head [28]. In order to determine the spatial relationship between IZUMO1R, CD9, and cytosolic PTK2B-PY^{402}, the fixed oocyte had to be permeabilized by TX100 to provide antibody access to the cytoplasmic compartment. TX-100 solubilized most of the oocyte surface IZUMO1R; however, IZUMO1R was retained at sperm binding sites, probably a result of protein–protein interactions unique to these sites.

Taken together, the above observations indicate that PTK2B phosphorylation begins at the early stages of sperm–oocyte binding. During this initial stage, IZUMO1R, CD9, and PTK2B-PY^{402} remain closely associated. However, as IZUMO1R was displaced laterally in response to IZUMO dimerization, CD9 and PTK2B-PY^{402} remained concentrated underneath the sperm head. As the oocyte cortex invaginated prior to sperm incorporation, CD9 and PTK2B-PY^{402} remained concentrated at the invagination site suggesting a role in the invagination process.

Role of IZUMO1R and CD9 in PTK2B recruitment and activation

In order to determine whether IZUMO1R or CD9 played a significant role in PTK2B recruitment and activation by bound sperm, knockout models were used to test the impact of *Izumo1r* or *Cd9* ablation on PTK2B distribution and activation. PTK2B was recruited to sperm binding sites in *Izumo1r*$^{-/-}$ as well as *Cd9*$^{-/-}$ oocytes indicating that neither protein is required for PTK2B recruitment. However, activation of PTK2B was highly dependent on the presence of CD9. Together, these observations indicate that IZUMO1R has a significant but minor role in activation of PTK2B while CD9 plays an essential role. The mechanism by which CD9 confers the ability of oocytes to respond to sperm binding via PTK2B activation remains an open question. While CD9 was shown to act as a cell surface receptor in some systems [43], such interactions are rare [44] and as yet, no sperm membrane proteins are known to act as ligands for CD9 [35]. More recently, a scenario has been proposed in which CD9-defined microdomains promote concentration and ligation of integrins or other sperm binding proteins to constitute a high-affinity sperm binding site [37]. While some evidence exists supporting interaction between PTK2B and the C-terminal region of integrin beta3, this interaction did not impact PTK2B activation [45]. However, it remains possible that the properties of CD9-maintained microdomains might facilitate dimerization of PTK2B leading to its activation by transphosphorylation. Since PTK2B activation also involves phosphorylation of Y^{402} by a *Src*-family kinase, recruitment of this kinase to the sperm binding site [46] might also play a role in PTK2B regulation. Future analyses will hopefully identify other components of the sperm binding site that interact directly with PTK2B or indirectly through other signaling pathways.

Role in actin remodeling. PTK2B is thought to play a role in meiotic spindle function [47]; however, the only known function of PTK2B during fertilization is its role in f-actin accumulation at sperm

binding sites, and that it promotes but is not absolutely required for sperm incorporation [4]. The finding that $Cd^{-/-}$ oocytes exhibited significantly reduced ability to activate PTK2B and accumulate f-actin at the sperm binding site indicates that CD9 is critical for both events. The specific mechanism through which PTK2B activation could impact actin remodeling is not well understood in any of the models studied thus far. For example, $PTK2B^{-/-}$ macrophages exhibit compromised Rho GTPase activity [12], but others have proposed that PTK2B inhibits the RhoA GTPase activating protein (Graf1c) in neurons [48]. Still other studies suggest that PTK2B may act downstream of integrin signaling during vascular smooth muscle contraction [15].

Possible ways by which CD9-dependent PTK2B activation might contribute to the fertilization process include a role in microvillus elongation enhancing surface contact area and sperm binding strength [41], and reorganization of oocyte membrane proteins within the sperm binding site, including cortex invagination prior to sperm engulfment [28]. Further analysis of actin-modulating proteins active at the sperm binding site of *wt* and $PTK2B^{-/-}$ oocytes will be required to understand this important aspect of sperm incorporation.

Summary

The present study has tested the role of IZUMO1R and CD9 in activation of PTK2B and remodeling of the cortical actin layer within the oocyte. Imaging studies demonstrated that, while the level of activated PTK2B at sperm binding sites correlated positively with the amount of IZUMO1R and CD9, activated PTK2B was localized most closely with CD9 throughout the membrane rearrangements that occur at the sperm binding site. Functional studies revealed that while *Izumo1r* ablation suppressed PTK2B activation by approximately 50%, it had no adverse effect on f-actin accumulation at the sperm binding site. In contrast, *Cd9* expression played a critical role enabling both PTK2B activation and f-actin accumulation at the sperm binding site. While we have no evidence of CD9 binding to PTK2B, these results are consistent with a model where CD9 or other membrane proteins enriched in a CD9-maintained membrane domain could trigger PTK2B activation at the sperm binding site. Further analysis of the membrane proteins comprising the sperm binding site and their interactions with cytoplasmic signaling proteins such as PTK2B is needed before this complex aspect of fertilization is understood.

Data Availability

Images and associated image analysis data will be deposited in the Image Data Resource "https://doi.org/10.1038/nmeth.4326".

Supplementary material

Supplementary material is available at *BIOLRE* online.

Acknowledgements

We wish to thank Dr. E. Bianchi and G. Wright (Wellcome Trust Sanger Institute; Cambridge, UK) for helpful discussions and for providing the $Izumo1r^{-/-}$ mouse line, Dr. Sara Wells for assistance for insightful contributions to the discussion, and Karen Kinsey for development of an excel program for image analysis.

Conflict of interest

The authors have declared that no conflict of interest exists.

References

1. Cline CA, Schatten H, Balczon R, Schatten G. Actin-mediated surface motility during sea urchin fertilization. *Cell Motil* 1983; **3**:513–524.
2. Tilney LG, Jaffe LA. Actin, microvilli, and the fertilization cone of sea urchin eggs. *J Cell Biol* 1980; **87**:771–782.
3. Kumakiri J, Oda S, Kinoshita K, Miyazaki S. Involvement of rRho family G protein in the cell signaling for sperm incorporation during fertilization of mouse eggs: inhibition by Clostridium difficile toxin B. *Dev Biol* 2003; **260**:522–535.
4. Wang H, Luo J, Carlton C, McGinnis LK, Kinsey WH. Sperm-oocyte contact induces outside-in signaling via PTK2B activation. *Dev Biol* 2017; **428**:52–62.
5. Shi CS, Kehrl JH. PTK2B amplifies epidermal growth factor and c-Src-induced Stat 3 activation. *J Biol Chem* 2004; **279**:17224–17231.
6. Kodama H, Fukuda K, Takahashi T, Sano M, Kato T, Tahara S, Hakuno D, Sato T, Manabe T, Konishi F, Ogawa S. Role of EGF receptor and PTK2B in endothelin-1-induced ERK activation in rat cardiomyocytes. *J Mol Cell Cardiol* 2002; **34**:139–150.
7. Yang CM, Lee IT, Hsu RC, Chi PL, Hsiao LD. NADPH oxidase/ROS-dependent PTK2Bactivation is involved in TNF-alpha-induced matrix metalloproteinase-9 expression in rat heart-derived H9c2 cells. *Toxicol Appl Pharmacol* 2013; **272**:431–442.
8. Butler B, Blystone SD. Tyrosine phosphorylation of beta 3 integrin provides a binding site for PTK2B. *J Biol Chem* 2005; **280**:14556–14562.
9. van Buul, Anthony EC, Fernandez-Borja M, Burridge K, Hordijk PL. Proline-rich tyrosine kinase 2 (PTK2B) mediates vascular endothelial-cadherin-based cell-cell adhesion by regulating beta-catenin tyrosine phosphorylation. *J Biol Chem* 2005; **280**:21129–21136.
10. Lev S, Moreno H, Martinez R, Canoll P, Peles E, Musacchio JM, Plowman GD, Rudy B, Schlessinger J. Protein tyrosine kinase PTK2B involved in Ca(2+)-induced regulation of ion channel and MAP kinase functions. *Nature* 1995; **376**:737–745.
11. Matsubara T, Yaginuma T, Addison WN, Fujita Y, Watanabe K, Yoshioka I, Hikiji H, Maki K, Baron R, Kokabu S. Plectin stabilizes microtubules during osteoclastic bone resorption by acting as a scaffold for Src and PTK2B. *Bone* 2019; **132**:115209.
12. Okigaki M, Davis C, Falasca M, Harroch S, Felsenfeld DP, Sheetz MP, Schlessinger J. PTK2B regulates multiple signaling events crucial for macrophage morphology and migration. *Proc Natl Acad Sci USA* 2003; **100**:10740–10745.
13. Owen KA, Thomas KS, Bouton AH. The differential expression of Yersinia pseudotuberculosis adhesins determines the requirement for FAK and/or PTK2B during bacterial phagocytosis by macrophages. *Cell Microbiol* 2007; **9**:596–609.
14. Koppel AC, Kiss A, Hindes A, Burns CJ, Marmer BL, Goldberg G, Blumenberg M, Efimova T. Delayed skin wound repair in proline-rich protein tyrosine kinase 2 knockout mice. *Am J Physiol Cell Physiol* 2014; **306**:C899–C909.
15. Mills RD, Mita M, Nakagawa J, Shoji M, Sutherland C, Walsh MP. A role for the tyrosine kinase PTK2B in depolarization-induced contraction of vascular smooth muscle. *J Biol Chem* 2015; **290**:8677–8692.
16. Tong L, Ao JP, Lu HL, Huang X, Zang JY, Liu SH, Song NN, Huang SQ, Lu C, Chen J, Xu WX. Tyrosine kinase PTK2B is involved in colonic smooth muscle contraction via the RhoA/ROCK pathway. *Physiol Res* 2019; **68**:89–98.
17. Fan L, Lu Y, Shen X, Shao H, Suo L, Wu Q. Alpha protocadherins and PTK2B kinase regulate cortical neuron migration and cytoskeletal dynamics via Rac1 GTPase and WAVE complex in mice. *Elife* 2018; **7**:001.
18. Evans JP. Sperm-egg interaction. *Annu Rev Physiol* 2012; **74**:477–502.
19. Barraud-Lange V, Naud-Barriant N, Saffar L, Gattegno L, Ducot B, Drillet AS, Bomsel M, Wolf JP, Ziyyat A. Alpha 6beta1 integrin expressed by sperm is determinant in mouse fertilization. *BMC Dev Biol* 2007; **7**:102.
20. Miyado K, Yamada G, Yamada S, Hasuwa H, Nakamura Y, Ryu F, Suzuki K, Kosai K, Inoue K, Ogura A, Okabe M, Mekada E. Requirement of CD9 on the egg plasma membrane for fertilization. *Science* 2000; **287**:321–324.

21. Le Naour, Rubinstein E, Jasmin C, Prenant M, Boucheix C. Severely reduced female fertility in CD9-deficient mice. *Science* 2000; **287**:319–321.
22. Barraud-Lange V, Naud-Barriant N, Bomsel M, Wolf JP, Ziyyat A. Transfer of oocyte membrane fragments to fertilizing spermatozoa. *FASEB J* 2007; **21**:3446–3449.
23. Takahashi Y, Bigler D, Ito Y, White JM. Sequence-specific interaction between the disintegrin domain of mouse ADAM 3 and murine eggs: role of beta 1 integrin-associated proteins CD9, CD81, and CD98. *Mol Biol Cell* 2001; **12**:809–820.
24. Coonrod SA, Naaby-Hansen S, Shetty J, Shibahara H, Chen M, White JM, Herr JC. Treatment of mouse oocytes with PI-PLC releases 70-kDa (pI 5) and 35- to 45-kDa (pI5.5) protein clusters from the egg surface and inhibits sperm-oolemma binding and fusion. *Dev Biol* 1999; **207**:334–349.
25. Bianchi E, Doe B, Goulding D, Wright GJ. IZUMO1R is the egg IZUMO receptor and is essential for mammalian fertilization. *Nature* 2014; **508**:483–487.
26. Zhao M, Finlay D, Zharkikh I, Vuori K. Novel role of Src in priming PTK2B phosphorylation. *PLoS One* 2016; **11**:e0149231.
27. Miyado K, Yoshida K, Yamagata K, Sakakibara K, Okabe M, Wang X, Miyamoto K, Akutsu H, Kondo T, Takahashi Y, Ban T, Ito C et al. The fusing ability of sperm is bestowed by CD9- containing vesicles released from eggs in mice. *Proc Natl Acad Sci USA* 2008; **105**:12921–12926.
28. Inoue N, Hagihara Y, Wright D, Suzuki T, Wada I. Oocyte-triggered dimerization of sperm IZUMO1 promotes sperm-egg fusion in mice. *Nat Commun* 2015; **6**:8858.
29. Kaji K, Oda S, Shikano T, Ohnuki T, Uematsu Y, Sakagami J, Tada N, Miyazaki S, Kudo A. The gamete fusion process is defective in eggs of Cd9-deficient mice. *Nat Genet* 2000; **24**:279–282.
30. Chalbi M, Barraud-Lange V, Ravaux B, Howan K, Rodriguez N, Soule P, Ndzoudi A, Boucheix C, Rubinstein E, Wolf JP, Ziyyat A, Perez E et al. Binding of sperm protein Izumo1 and its egg receptor IZUMO1R drives Cd9 accumulation in the intercellular contact area prior to fusion during mammalian fertilization. *Development* 2014; **141**:3732–3739.
31. Ravaux B, Favier S, Perez E, Gourier C. Egg CD9 protein tides correlated with sperm oscillations tune the gamete fusion ability in mammal. *J Mol Cell Biol* 2018; **10**:494–502.
32. Satouh Y, Inoue N, Ikawa M, Okabe M. Visualization of the moment of mouse sperm-egg fusion and dynamic localization of IZUMO1. *J Cell Sci* 2012; **125**:4985–4990.
33. Santella L, Limatola N, Vasilev F, Chun JT. Maturation and fertilization of echinoderm eggs: role of actin cytoskeleton dynamics. *Biochem Biophys Res Commun* 2018; **506**:361–371.
34. Shalgi R, Phillips D. Mechanics of sperm entry in cycling hamsters. *J Ultrastruct Res* 1980; **71**:154–161.
35. Vjugina U, Evans JP. New insights into the molecular basis of mammalian sperm-egg membrane interactions. *Front Biosci* 2008; **13**: 462–476.
36. Barbaux S, Ialy-Radio C, Chalbi M, Dybal E, Homps-Legrand M, Do Cruzeiro, Vaiman D, Wolf JP, Ziyyat A. Sperm SPACA6 protein is required for mammalian sperm-egg adhesion/fusion. *Sci Rep* 2020; **10**:5335.
37. Jegou A, Ziyyat A, Barraud-Lange V, Perez E, Wolf JP, Pincet F, Gourier C. CD9tetraspanin generates fusion competent sites on the egg membrane for mammalian fertilization. *Proc Natl Acad Sci USA* 2011; **108**:10946–10951.
38. Hall JE, Fu W, Schaller MD. Focal adhesion kinase: exploring Fak structure to gain insight into function. *Int Rev Cell Mol Biol* 2011; **288**:185–225.
39. van Seventer, Mullen MM, van Seventer. PTK2B is differentially regulated bybeta1 integrin- and CD28-mediated co-stimulation in human CD4+ T lymphocytes. *Eur JImmunol* 1998; **28**:3867–3877.
40. Jean C, Haghighirad F, Zhu Y, Chalbi M, Ziyyat A, Rubinstein E, Gourier C, Yip P, Wolf JP, Lee JE, Boucheix C, Barraud-Lange V. IZUMO1R, the receptor of sperm IZUMO1, is expressed by the human oocyte and is essential for human fertilisation. *Hum Reprod* 2019; **34**: 118–126.
41. Runge KE, Evans JE, He ZY, Gupta S, McDonald KL, Stahlberg H, Primakoff P, Myles DG. Oocyte CD9 is enriched on the microvillar membrane and required for normal microvillar shape and distribution. *Dev Biol* 2007; **304**:317–325.
42. Benammar A, Ziyyat A, Lefevre B, Wolf JP. Tetraspannins and mouse oocyte microvilli related to fertilizing ability. *Reprod Sci* 2017; **24**:1062–1069.
43. Waterhouse R, Ha C, Dveksler GS. Murine CD9 is the receptor for pregnancy-specific glycoprotein 17. *J Exp Med* 2002; **195**:277–282.
44. Reyes R, Cardenes B, Machado-Pineda Y, Cabanas C. Tetraspannin CD9: a key regulator of cell adhesion in the immune system. *Front Immunol* 2018; **9**:863.
45. Pfaff M, Jurdic P. Podosomes in osteoclast-like cells: structural analysis and cooperative roles of paxillin, proline-rich tyrosine kinase 2 (PTK2B) and integrin alpha Vbeta3. *J Cell Sci* 2001; **114**:2775–2786.
46. Townley IK, Schuyler E, Parker-Gur M, Foltz KR. Expression of multiple Src family kinases in sea urchin eggs and their function in Ca^{2+} release at fertilization. *Dev Biol* 2009; **327**:465–477.
47. Meng XQ, Cui B, Cheng D, Lyu H, Jiang LG, Zheng KG, Liu SZ, Pan J, Zhang C, Bai J, Zhou J. Activated proline-rich tyrosine kinase 2 regulates meiotic spindle assembly in the mouse oocyte. *J Cell Biochem* 2018; **119**:736–747.
48. Lee S, Salazar SV, Cox TO, Strittmatter SM. PTK2B Signaling through Graf1 and RhoAGTPase is required for amyloid-beta oligomer-triggered synapse loss. *J Neurosci* 2019; **39**:1910–1929.